Extended Structures and Magnetic Properties of Lanthanide–Copper Complexes with Picolinic Acids as Bridging Ligands

A-Qing Wu,[a] Guang-Hua Guo,[a] Chun Yang,[a] Fa-Kun Zheng,[a] Xi Liu,[a] Guo-Cong Guo,*[a] Jin-Shun Huang,[a] Zhen-Chao Dong,*[b] and Yoshihiko Takano[c]

Keywords: Heterometallic complexes / Magnetic properties / Crystal structures / Picolinic acid / Coordination polymers

The first examples of 3d–4f heterometallic complexes containing picolinic acid ligands were synthesized and characterized. Three series of complexes were obtained by the reaction of presynthesized "metallo ligands" $Cu(pic)_2$ and $Ln(ClO_4)_3$ in 2:1, 3:1, and 4:1 mole ratios. Complexes **1**–**3** (denoted as the first series), $[LnCu_2(pic)_4(H_2O)_6](ClO_4)_3{\cdot}H_2O$ (Ln = Sm, Nd, and Pr), are isomorphous and exhibit infinite 1D zigzag chain structures with rare earth ions in tricapped trigonal prismatic coordination. Complexes **4**–**10** (denoted as the second series), $[Ln_2Cu_5(pic)_{10}(H_2O)_8](ClO_4)_6{\cdot}2H_2O$ (Ln = Gd, Nd, Sm, Dy, Eu, Pr, and Yb), are isomorphous too, and exhibit extended 2D layered structures constituted by $Cu(pic)_2$ moieties bridging the zigzag chains. Complex **11** (denoted as the third-type complex), $\{NdCu(pic)_2[CO(NH_2)_2]_4(H_2O)_3\}(ClO_4)_3{\cdot}[Cu(pic)_2]_2$, exhibits another type of nearly linear chain structure with additional $Cu(pic)_2$ moieties trapped in the lattice by hydrogen bonds. Temperature-dependent magnetizations of complexes **2**–**4**, **6**, and **11** indicate that these complexes follow the Curie–Weiss paramagnetic behavior down to 5 K.

Introduction

Studies on the syntheses, structures and properties of 3d–4f heterometallic complexes are currently of great interest because they are good models for the investigation of the nature of the magnetic interactions between 3d and 4f metal ions in magnetic materials.[1] The main synthetic strategy for 3d–4f complexes is to use bridging ligands to link 3d and 4f paramagnetic building blocks to generate discrete polynuclear or extended topological complexes of high dimensionalities, while the latter may enhance and improve bulk magnetic properties due to the increased number of interacting neighbors.[2] Since the Ln and M (M = transition metal) ions may be connected through bidentate carboxylate groups, efforts have been made to use carboxylate acids and carboxylate-like betaines as ligands. Many such studies focused on discrete polynuclear complexes such as LnM, LnM_2, Ln_2M_2, Ln_2M_4, Ln_2M_8 etc.[3–7] In comparison, multidimensional heterometallic complexes are relatively rare,[8] and the synthesis of the multidimensional 3d–4f complexes is still a great challenge. An effective strategy employed is the use of relatively stable metal complexes containing potential coordinating atoms, that is "metallo ligands", to link rare earth ions to form polymeric networks. This strategy is called stepwise synthesis.[4b,9] In our laboratory, we have synthesized a series of polymeric 3d–4f complexes through the use of carboxylate groups as bridging units.[10] As an extension of this work, picolinic acid (Hpic) was used as a chelating ligand to make the $[COH(NH_2)_2]_2[Cu(pic)_2(ClO_4)_2]$ precursor by reaction with $Cu(ClO_4)_2$;[11] The monomer $Cu(pic)_2$ can be used as a "metallo ligand" to bind lanthanide metal ions for the preparation of complexes containing rare earth and transition metals. We have successfully obtained three novel series of one- and two-dimensional 3d–4f coordination polymers, namely, $[LnCu_2(pic)_4(H_2O)_6](ClO_4)_3{\cdot}H_2O$ [Ln = Sm (**1**), Nd (**2**), and Pr (**3**)] (1D), $[Ln_2Cu_5(pic)_{10}(H_2O)_8](ClO_4)_6{\cdot}2H_2O$ [Ln = Gd (**4**), Nd (**5**), Sm (**6**), Dy (**7**), Eu (**8**), Pr (**9**), and Yb (**10**)] (2D) and $\{NdCu(pic)_2[CO(NH_2)_2]_4(H_2O)_3\}(ClO_4)_3{\cdot}[Cu(pic)_2]_2$ (**11**) (1D). Although picolinic acid ligands were previously used to synthesize a number of metal complexes with transition metals or rare earths alone,[12] to the best of our knowledge, mixed multinuclear or multidimensional 3d–4f heterometallic complexes with picolinic acid ligands have not been reported. Herein, we report the syntheses and structures of **1**–**11**, as well as the magnetic properties of **2**–**4**, **6**, and **11**.

[a] State Key Laboratory of Structural Chemistry, Fujian Institute of Research on the Structure of Matter, Chinese Academy of Sciences,
Fuzhou, Fujian 350002, People's Republic of China
Fax: +86-591-3714946
E-mail: gcguo@ms.fjirsm.ac.cn
[b] Hefei National Laboratory for Physical Sciences at Microscale, University of Science and Technology of China,
96 Jinzhai Road, Hefei, Anhui 230026, People's Republic of China
[c] National Institute for Materials Science,
1-2-1 Sengen, Tsukuba, Ibaraki 305–0047, Japan

Results and Discussion

Syntheses

In order to construct such extended 3d–4f heterometallic structures, an assembly reaction is designed to have the $Cu(pic)_2$ complex acting as a 3d-component precursor and $Ln(ClO_4)_3$ as a 4f-component. The $Cu(pic)_2$ complex with two non-coordinated oxygen atoms of carboxyl groups may function as a "metallo ligand" to the Ln^{III} component. In the course of the investigation, the one-dimensional chain complexes **1**–**3**, $[LnCu_2(pic)_4(H_2O)_6](ClO_4)_3{\cdot}H_2O$, were obtained by the reaction of a 2:1 mole ratio of $Cu(pic)_2$ and $Ln(ClO_4)_3$ in C_2H_5OH/CH_3CN mixed solution at room temperature. Structural analyses indicate that the Ln^{III} atoms in **1**–**3** are surrounded by three $Cu(pic)_2$ moieties in a T-shape fashion to form a zigzag chain structure with large open spaces on the Ln ions (see Figure 1), which suggests that the Ln ions can be further coordinated by more $Cu(pic)_2$ ligands to form higher dimensional structures. On the basis of this idea, the mole ratio of $Cu(pic)_2$ to $Ln(ClO_4)_3$ was increased to 3:1, and seven expected two-dimensional heterometallic isomorphs, $[Ln_2Cu_5(pic)_{10}(H_2O)_8](ClO_4)_6{\cdot}2H_2O$ (**4**–**10**), were successfully obtained. However, we failed to synthesize a three-dimensional heterometallic complex by further increasing the mole ratio to 4:1 with the addition of more carbamide to maintain the pH at 5. Instead, a new structure with a nearly linear one-dimensional chain, $\{NdCu(pic)_2[CO(NH_2)_2]_4(H_2O)_3\}(ClO_4)_3{\cdot}[Cu(pic)_2]_2$ (**11**), showed up with "superfluous" $Cu(pic)_2$ moieties trapped in the lattice. The failure may be related to the large steric effect of $Cu(pic)_2$ ligands and competition coordination of carbamide.

Crystal Structures

The crystal structures of **1**–**11** were determined by single-crystal X-ray diffraction analyses. The crystallographic data are summarized in Table 1 for **1**–**3**, Table 2 for **4**–**6**, Table 3 for **7**–**9**, and Table 4 for **10** and **11**. Complexes **1**–**3** and **4**–**10** are isomorphous, so we chose complexes **1**, **4,** and **11** to

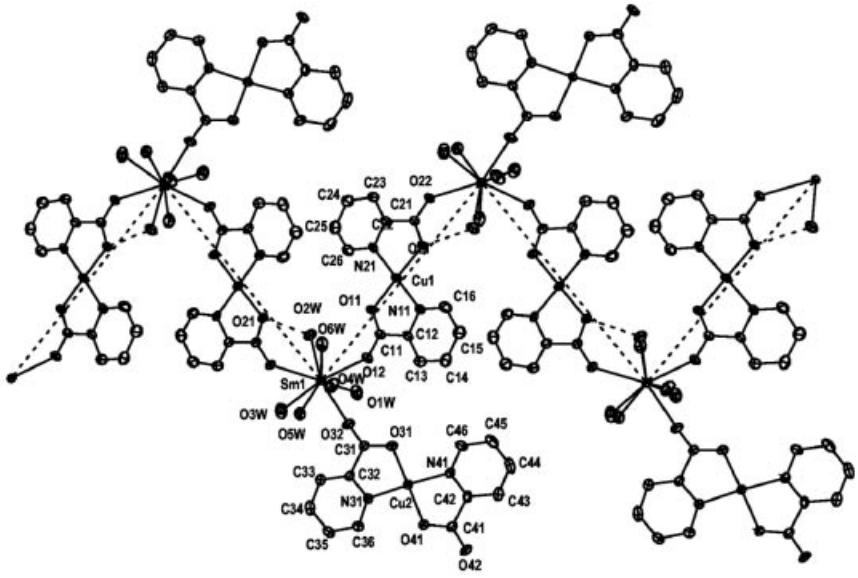

Figure 1. The chain structure of **1** extending along the *b* direction with 35% thermal ellipsoids.

Table 1. Crystal data and structure refinements for complexes **1**–**3**.

Complex $LnCu_2(pic)_4(H_2O)_6$ $(ClO4)_3{\cdot}H_2O$	**1** ($SmCu_2$)	**2** ($NdCu_2$)	**3** ($PrCu_2$)
Formula	$C_{24}H_{30}Cl_3Cu_2N_4O_{27}Sm$	$C_{24}H_{30}Cl_3Cu_2N_4NdO_{27}$	$C_{24}H_{30}Cl_3Cu_2N_4O_{27}Pr$
Fw	1190.30	1184.19	1180.86
Space group	*Pcab*	*Pcab*	*Pcab*
a [Å]	13.690(2)	13.7095(1)	13.7046(3)
b [Å]	14.8425(6)	14.8578(2)	14.8745(1)
c [Å]	39.3740(6)	39.4425(4)	39.4457(7)
V [Å^3]	8000.5(11)	8034.2(2)	8041.0(2)
Z	8	8	8
ρ [g cm^{-3}]	1.973	1.975	1.951
μ [mm^{-1}]	2.635	2.793	2.541
λ [Å]	0.71073	0.71073	0.71073
T [K]	293(2)	293(2)	293(2)
R_1,wR_2 (obs.)	0.0569, 0.1558	0.0583, 0.1323	0.0666, 0.1553
Goodness of fit	1.023	1.037	1.091

Table 2. Crystal data and structure refinements for complexes **4**–**6**.

Complex $[Ln_2Cu_5(pic)_{10}(H_2O)_8]\cdot 6[ClO_4]\cdot 2H_2O$	Gd_2Cu_5	Nd_2Cu_5	Sm_2Cu_5
Formula	$C_{60}H_{60}Cl_6Cu_5Gd_2N_{10}O_{54}$	$C_{60}H_{60}Cl_6Cu_5N_{10}Nd_2O_{54}$	$C_{60}H_{60}Cl_6Cu_5N_{10}O_{54}Sm_2$
Fw	2630.08	2604.06	2616.28
Space group	$P\bar{1}$	$P\bar{1}$	$P\bar{1}$
a [Å]	8.7129(17)	8.721(2)	8.7205 (1)
b [Å]	14.900(3)	14.9145 (1)	14.9373 (1)
c [Å]	16.791(3)	16.8147(2)	16.8181 (1)
α [°]	81.59(3)	81.563(1)	81.612 (1)
β [°]	86.29(3)	86.260(1)	86.449 (1)
γ [°]	84.59(3)	84.621(1)	84.614 (1)
V [Å^3]	2143.9(7)	2150.84(3)	2155.14(3)
Z	1	1	1
ρ [g cm^{-3}]	2.037	2.010	2.016
μ [mm^{-1}]	3.043	2.699	2.851
λ [Å]	0.71073	0.71073	0.71073
T [K]	293(2)	293(2)	293(2)
R_1, wR_2 (obs.)	0.0408, 0.1106	0.0629, 0.1584	0.0386, 0.0926
Goodness of fit	1.027	1.038	1.040

Table 3. Crystal data and structure refinements for complexes **7**–**9**.

Complex $[Ln_2Cu_5(pic)_{10}(H_2O)_8]\cdot 6[ClO_4]\cdot 2H_2O$	Dy_2Cu_5	Eu_2Cu_5	Pr_2Cu_5
Formula	$C_{60}H_{60}Cl_6Cu_5Dy_2N_{10}O_{54}$	$C_{60}H_{60}Cl_6Cu_5Eu_2N_{10}O_{54}$	$C_{60}H_{60}Cl_6Cu_5N_{10}O_{54}Pr_2$
Fw	2640.58	2619.50	2597.40
Space group	$P\bar{1}$	$P\bar{1}$	$P\bar{1}$
a [Å]	8.71790(10)	8.7140(2)	8.68860(10)
b [Å]	14.9062(3)	14.8939(3)	14.8669(1)
c [Å]	16.8218(3)	16.7935(4)	16.7575(3)
α [°]	81.5480(10)	81.6600(10)	81.5770(10)
β [°]	86.2290(10)	86.3550(10)	86.315(1)
γ [°]	84.4550(10)	84.5680(10)	84.6630(10)
V [Å^3]	2149.19(6)	2144.07(8)	2129.16(5)
Z	1	1	1
ρ [g cm^{-3}]	2.040	2.029	2.037
μ [mm^{-1}]	3.231	2.959	2.652
λ [Å]	0.71073	0.71073	0.71073
T [K]	293(2)	293(2)	293(2)
R_1, wR_2 (obs.)	0.0412, 0.0889	0.0519, 0.0989	0.0650, 0.1499
Goodness of fit	1.062	1.071	1.080

represent the three series for detailed structure discussions. The structural details of the other complexes, **2**, **3**, and **5**–**10**, are deposited with the CCDC.

Table 4. Crystal data and structure refinements for complexes **10** and **11**.

Complex	Yb_2Cu_5	NdCu
Formula	$C_{60}H_{60}Cl_6Cu_5Dy_2N_{10}O_{54}$	$C_{40}H_{46}Cl_3Cu_3N_{14}NdO_{31}$
Fw	2661.66	1660.12
Space group	$P\bar{1}$	$P2_1/c$
a [Å]	8.67570(10)	10.514(2)
b [Å]	14.8466(3)	22.311(5)
c [Å]	16.7580(1)	25.781(5)
α [°]	81.346(1)	90
β [°]	85.909(1)	96.35(3)
γ [°]	84.322(1)	90
V [Å^3]	2119.96(5)	6011(2)
Z	1	4
ρ [g cm^{-3}]	2.085	1.835
μ [mm^{-1}]	3.719	2.133
λ [Å]	0.71073	0.71073
T [K]	293(2)	293(2)
R_1, wR_2 (obs.)	0.0334, 0.0732	0.0614, 0.1709
Goodness of fit	1.064	1.016

$[LnCu_2(pic)_4(H_2O)_6](ClO_4)_3\cdot H_2O$ [Ln = Sm (1), Nd (2), and Pr (3)]

Complex **1** consists of one-dimensional chain $\{[SmCu_2(pic)_4(H_2O)_6]^{3+}\}_\infty$ cations, $[ClO_4]^-$ anions, and lattice water molecules, as shown in Figure 1. The coordination polyhedron of the nine-coordinate Sm atom can be described as a distorted tricapped trigonal prism, which is constructed by three carboxylic oxygen atoms from $Cu(pic)_2$ moieties and six water oxygen atoms. The two trigonal surfaces are both defined by two water O atoms and one carboxylic oxygen atom of one $Cu(pic)_2$ moiety (O2W, O6W and O12 atoms for the top surface, and O3W, O5W and O32 atoms for the bottom surface), while the three capping atoms are occupied by the remaining three coordinated oxygen atoms (O1W, O4W and O22), the Sm^{III} atom deviating from the plane by 0.034(1) Å. The O(cap)-Sm-O(cap) bond angles are 119.41(6) ° for O1W–Sm1–O22, 124.8 ° for O1W–Sm1–O4W, and 115.72(6) ° for O22–Sm–O4W; these are close to 120 ° in a regular triangle. The average Sm–O(prism) bond

lengths of 2.471(2) Å are shorter than average Sm–O(cap) bond lengths of 2.556(2) Å, as in the case found in Ln complexes.[13,10] The Ln–O bond lengths in **1**–**3** become shorter with increasing atomic number of Ln, because of the lanthanide contraction.

The $Cu(pic)_2$ moieties are nearly coplanar with a maximal deviation of 0.093(4) Å of Cu(2) in the $Cu(2)(pic)_2$ moiety, in which the Cu^{II} atom possesses an approximate centro-symmetric square-planar coordination environment, chelated by two picolinic acid ligands through the nitrogen atoms and carboxylic oxygen atoms of pic ligands. Four donor atoms N_2O_2 of pic ligands form a rectangle with angles close to 90 ° (88.01–92.48 °). The average Cu–N and Cu–O bond lengths are 1.972(3) and 1.940(2) Å, respectively; these lengths are consistent with those found in the $Cu(pic)_2$ complex reported previously.[11]

The Sm^{III} centers act as two-connected nodes and are bridged by two uncoordinated carboxylic O atoms of $Cu(1)(pic)_2$ moieties to form an infinite zigzag 1D chain extending along the *b* direction with the angle Cu1–Sm–Cu1 = 78.474(4) ° and Sm–Cu1–Sm = 174.89(1)° (Figure 1). Simultaneously, there exists a kind of intramolecular hydrogen bond between the atoms O21 and O2W (O2W···O21#A = 2.725(2) Å, symmetry code #A: *x*, –0.5 + *y*, 0.5 – *z*) as shown in Figure 2. The $Cu(2)(pic)_2$ moiety acts as a terminal ligand coordinated to the Sm^{III} ion through one of two uncoordinated carboxylic oxygen atoms. The Sm^{III} and Cu^{II} ions in the chain are nearly coplanar. The shortest intrachain Sm···Cu, Cu···Cu, and Sm···Sm separations are 5.8524(6), 7.4301(3), and 11.7349(5) Å, respectively. The adjacent chains are linked into two-dimensional structure along the *c* direction by intermolecular hydrogen bonds of O1W···O42#B and O5W···O42#B (symmetry code #B: –*x*, 1 – *y*, –*z*) with an average length of 2.837(3) Å, as shown in Figure 2. In each layer, there also exist π–π stacking interactions between the pyridine rings of the terminal coordinated $Cu(2)(pic)_2$ moieties from the adjacent chains with the centroid-centroid distance of 3.766 Å and the dihedral angle of 2.39 °. The lattice water molecules and ClO_4^- anions with hydrogen bonds among them are located between the layers (O7W···O16#C = 3.046 Å; O7W···O33#C = 3.051 Å, symmetry code #C: *x* – 1, *y*, *z*). These lattice molecules form hydrogen bonds with the coordinated water molecules in the layer. These hydrogen bonds bridge the layers to form a three-dimensional framework along the *a* direction. Such π–π stacking and hydrogen bonding interactions lead to the stabilization of the crystal structure.

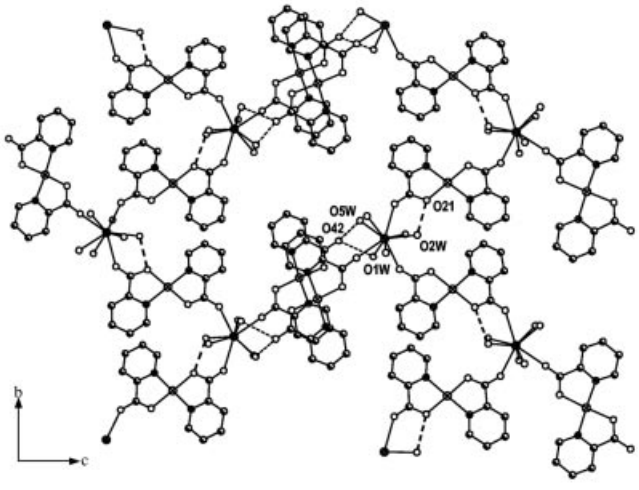

Figure 2. The hydrogen bonding and π–π stacking interactions link the chains into a layer-like structure in **1** along the *c* axis. The intermolecular hydrogen bonds are represented by the thin dashed lines and the intramolecular hydrogen bonds by the thick dashed lines.

[$Ln_2Cu_5(pic)_{10}(H_2O)_8$][$(ClO_4)_6$·$2H_2O$ [Ln = Gd (4), Nd (5), Sm (6), Dy (7), Eu (8), Pr (9) and Yb (10)]

Figure 3 shows the structure of **4** with the asymmetric atoms labeled. The coordination polyhedron of eight-coordinate Gd^{III} can be viewed as a distorted square antiprism, formed by the four carboxylic oxygen atoms from four picolinic acid ligands and four neutral water molecules. One square plane is defined by three water O atoms and one carboxylic oxygen atom of one $Cu(pic)_2$ moiety (O1W, O2W, O3W and O2) with a maximal deviation of 0.059 Å of the O2 atom, while the other square plane is defined by one water O atom and three carboxylic oxygen atoms from three different $Cu(pic)_2$ moieties (O4W, O22, O32, and O42) with a maximal deviation of 0.145 Å of the O22 atom. The O–O–O bond angles in the two square planes range from 81.31 to 98.45 °, they are close to 90 ° for a regular square. The two square planes are nearly parallel with the dihedral angle of 6.63 °. The Gd–O bond lengths are almost identical with a maximal difference of 0.14 Å.

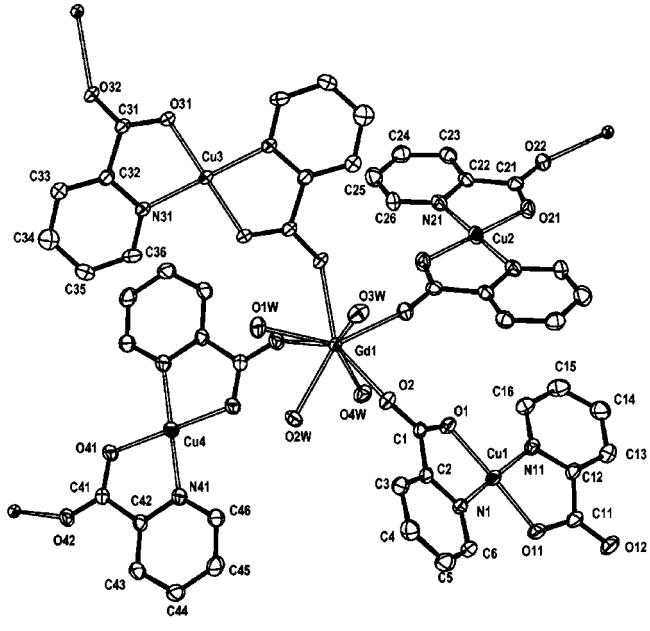

Figure 3. Basic structure unit of **4** with 30% thermal ellipsoids.

There are four $Cu(pic)_2$ units around each Gd^{III}, as shown in Figure 3. The Gd^{III} atoms are linked by the unco-

ordinated carboxylic O atoms of the $Cu(4)(pic)_2$ and the $Cu(3)(pic)_2$ moieties to form a pseudozigzag chain along the *b* direction. These chains are further bridged by $Cu(2)(pic)_2$ moieties through their two uncoordinated carboxylic O atoms along the *c* direction to form extended two-dimensional layers (Figure 4). The $Cu(1)(pic)_2$ moiety acts as a terminal ligand to Gd^{III} through coordination by one of its two uncoordinated carboxylic oxygen atoms. The closest intralayer separations of Sm···Cu, Cu···Cu, and Sm···Sm are 5.755, 7.45, and 11.510 Å, respectively. The adjacent layers are indirectly connected by hydrogen bonds consisting of coordinated water molecules and oxygen atoms of perchlorate anions or lattice water molecules located between layers, with O···O distances ranging from 2.743(5) to 3.002(6) Å. Simultaneously, the lattice water molecules and oxygen atoms of perchlorate anions form hydrogen bonds among themselves with an O···O distance of 2.933(6) Å.

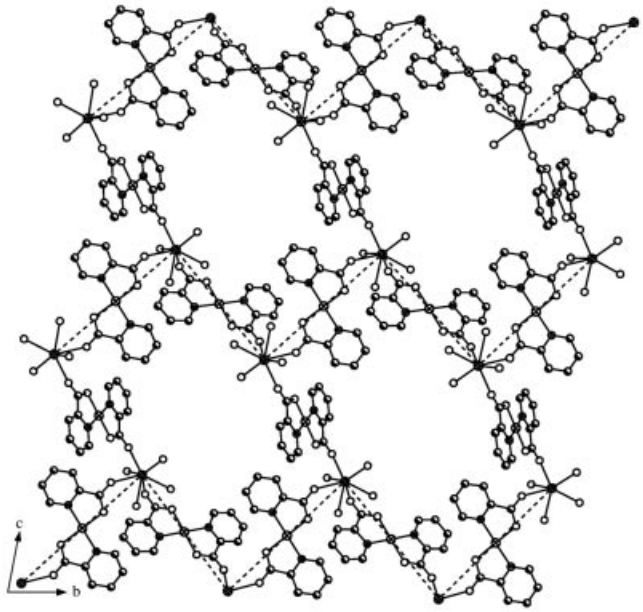

Figure 4. The layer sketch structure of **4** with the zigzag chain represented by dashed lines. Terminal $Cu(1)(pic)_2$ moieties were omitted for clarity.

{NdCu(pic)$_2$[CO(NH$_2$)$_2$]$_4$(H$_2$O)$_3$}(ClO$_4$)$_3$·[Cu(pic)$_2$]$_2$ (11)

Complex **11** consists of $\{NdCu(pic)_2[CO(NH_2)_2]_4(H_2O)_3\}_\infty$ cationic chains, ClO_4^- anions, and two lattice $Cu(pic)_2$ species. The coordination polyhedron of Nd^{III} can be viewed as a slightly distorted square antiprism, formed by two carboxylic oxygen atoms of two $Cu(pic)_2$ moieties (O2, O12), four oxygen atoms of carbamide (O13, O23, O33, O43), and two water oxygen atoms (O1W, O2W). One of the square planes consists of O12, O33, O43, and O2W atoms with a mean deviation of 0.01 Å from the least-squares plane, while O2, O13, O23, and O1W atoms form the other square plane with a mean deviation of 0.004 Å. The two square planes are nearly parallel with a dihedral angle of 5.75 °. The O–O–O bond angles in the two square planes range from 84.34 to 95.123 °. The Nd-O(pic) bond lengths are 2.496 Å for O2 and 2.537 Å for O12, which are longer than those in the reported Nd^{III} complex with the pic ligand (2.400–2.454 Å).[14] The Nd-O(carbamide) bond lengths are nearly identical, spanning a narrow range of 2.381–2.413 Å. The Nd^{III} ions are alternately bridged by $Cu(1)(pic)_2(H_2O)$ moieties through the O2 and O12 carboxylic oxygen atoms of picolinic acid ligands to form a nearly linear chain with a Cu–Nd–Cu angle of 171.32 ° and an Nd–Cu–Nd angle of 171.32 ° extending along the *a* direction, as shown in Figure 5. The closest intrachain Nd···Cu, Cu···Cu, and Nd···Nd separations are 5.326, 10.514, and 10.514 Å, respectively. Unlike the $Cu(pic)_2$ moieties in **1**–**10**, the Cu1 ion in **11** is five-coordinate by the four donor atoms of pic ligands, O1, O12, N1, and N11, and one water molecule (O3W) with a longer distance of 2.413(3) Å due to the Jahn–Tellller effects of the Cu^{II} atom. The O1, O12, N1, and N11 atoms form roughly a planar N_2O_2 with a maximal deviation of 0.145 Å and the copper ion is displaced from this plane toward the axial O3W by 0.183 Å. The average Cu1–O and Cu1–N bond lengths are 1.949 and 1.975 Å, respectively; these are also comparable with the normal value for copper(II) coordinated by pic ligands.[11]

The lattice $Cu(2)(pic)_2$ moieties and ClO_4^- ions are located between the chains. The lattice $Cu(2)(pic)_2$ moieties bridge the adjacent chains to form a double-chain structure through the hydrogen bonds of O21···O1W [2.914(2) Å], O32···O2W [2.738(3) Å] and O22···O3W [2.849(3) Å], while

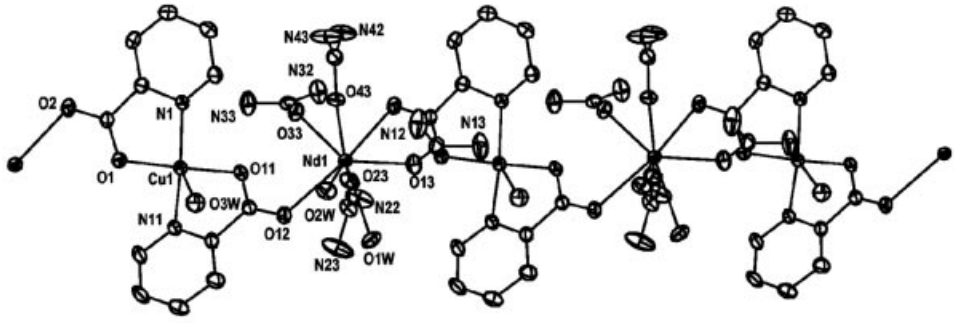

Figure 5. The nearly linear chain structure of **11** with 30% thermal ellipsoids.

the $Cl(3)O_4^-$ ions are anchored to the chains by hydrogen bonds of O34···O2W (2.797 Å) and O34···O3W (2.986 Å), as shown in Figure 6. In addition, there exist intramolecular hydrogen bonds between the N atom of one of coordinated urea molecules and O3W [N13···O2W = 3.023(3) Å] (Figure 6). The $Cu(3)(pic)_2$ moieties are located at two sides of the double chains.

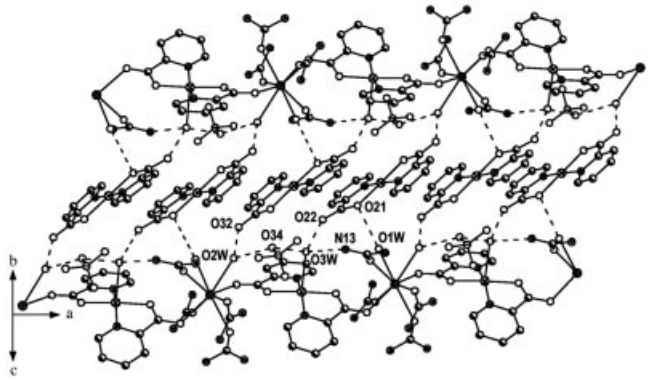

Figure 6. The double chain structure of **11** linked by the hydrogen bonds between lattice $Cu(2)(pic)_2$ moieties and carboxylic O atoms of single chains; the hydrogen bonds are represented by dashed lines.

The relations of mole ratios of different reactants and structures in the three series of complexes are shown in Scheme 1. The layered structures of the second series of complexes may be considered as being composed of the $Cu(pic)_2$ moieties bridging the zigzag chains in a similar manner to that of the first series complex. The Cu–Gd–Cu and Gd–Cu–Gd bond angles of the zigzag chain in **4** are 79.504 and 180.00 °, respectively, which are comparable to those of the first series of complexes [78.474(4) and 174.89(1) °, respectively]. The third series complex is very different from the former two series, in the sense that the $Cu(pic)_2$ moieties bridge lanthanide atoms in a nearly linear chain, with additional $Cu(pic)_2$ moieties serving as lattice molecules located in the lattice.

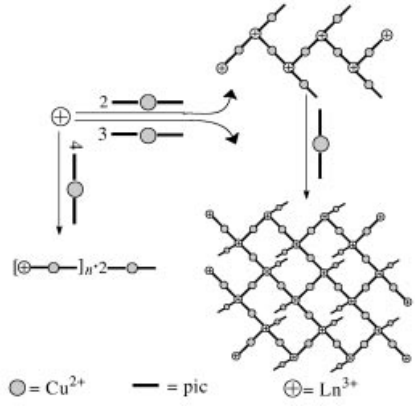

Scheme 1. The relations of mole ratios of different reactants and structures.

Magnetic Properties of Complexes 2–4, 6, and 11

The variable-temperature magnetic susceptibilities for crystalline samples **2**–**4**, **6**, and **11** were measured in the 6–300 K temperature range with an applied field of 1 T. Table 5 shows the non-linear fitting data to $\chi_M = C/(T - \theta) + \chi_0$ above 50 K and the effective magnetic moments, μ_{eff}, of all complexes, in which μ_{eff} is defined as $2.828C^{1/2}\mu_B$, χ_M the molar magnetic susceptibility, C the Curie constant, θ the Weiss constant, and χ_0 the background susceptibility. A Curie–Weiss paramagnetic behavior is observed for all these compounds. The observed effective magnetic moment for each compound is very close to the theoretical value at 293 K, expected for a coupling-free system of isolated Ln^{III} and Cu^{II} ions, which confirms the assignment of oxidation states as judged by the neutrality requirement. As shown in Figure 7, upon cooling, the $\chi_M'T$, where $\chi_M' = \chi_M - \chi_0$, decreases gradually from 300 to 15 K for all complexes. The nature of such antiferromagnetic-like behavior remains to be clarified for 4f–3d compounds, but it may be related to

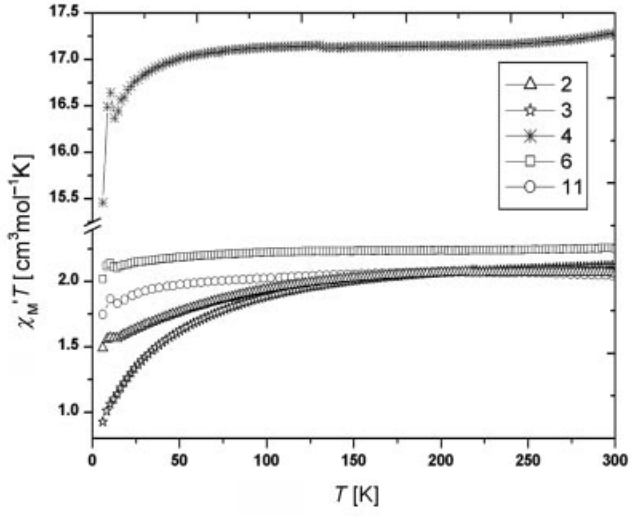

Figure 7. Thermal dependence of $\chi_M'T$ for complexes **2**–**4**, **6** and **11**.

Table 5. Magnetic fitting data of complexes **2**, **3**, **4**, **6**, and **11**.

Complexes	C [cm3 mol–1 K]	θ [K]	χ_0 [cm3 mol^{-1}]	μ_{eff}(exp.) (μ_B)	μ_{eff}(cal.) (μ_B)
$NdCu_2$ (**2**)	2.19(1)	–12.2(3)	$7.7(4)\times10^{-4}$	4.19(1)	4.371
$PrCu_2$ (**3**)	2.27(7)	–20.5(2)	$2(2)\times10^{-5}$	4.27(7)	4.333
Gd_2Cu_5 (**4**)	17.22(1)	–0.58(4)	$7(5)\times10^{-5}$	11.735(3)	11.873
Sm_2Cu_5 (**6**)	2.262(2)	–1.79(3)	$8.2(1)\times10^{-4}$	4.253(2)	4.047
NdCu (**11**)	2.091(7)	–3.0(2)	$5.1(3)\times10^{-4}$	4.261(7)	4.701

the progressive thermal depopulation of the Ln^{III} Stark components and a possible the Ln^{III}–Cu^{II} interaction.[15] Because of the large separation between the Ln^{III} ions and the well-shielded 4f orbitals by the outer shells of 5s and 5p orbitals as well as relatively low covalence of the lanthanide-to-ligand bonds, the Ln–Ln interactions are expected to be negligibly small. The origin of the small bumps around 15 K for **2**, **4**, **6**, and **11** is still unclear, though the possibility of a systematic error cannot be completely excluded. To date, the understanding of the magnetic interactions containing rare-earth ions in molecular magnets is still a challenge, particularly when the contribution of the first-order orbital momentum is involved. Further experiments are needed for better understanding of the nature of the 4f–3d magnetic interactions in these systems.

Conclusion

In summary, we have demonstrated a facile and controllable approach to 3d–4f heterometallic extended framework complexes. Firstly, we obtain one-dimensional array complexes in a T-shape fashion with a large open space on the other side. The introduction of more $Cu(pic)_2$ precursors into this open space leads to the formation of higher dimensional structures. A series of two-dimensional 3d–4f heterometallic complexes have been obtained in this way by increasing the mole ratio of metal complex precursor to Ln^{III} from 2:1 to 3:1. However, increasing the mole ratio further to 4:1 failed to yield three-dimensional heterometallic complexes, probably because of large steric effects of $Cu(pic)_2$ precursors and the competitive coordination of carbamide. Instead, an unexpected nearly linear heterometallic chain emerged. The present work may provide a useful approach to tuning structural dimensionality and thus magnetic properties through reactant mole ratios.

Experimental Section

Materials and Measurement: All starting reagents, except for $Ln(ClO_4)_3$ and $Cu(ClO_4)_2$, were commercial grade materials and used as received. $Ln(ClO_4)_3$ and $Cu(ClO_4)_2$ were prepared by the reactions of Ln_2O_3 or CuO and perchloric acid in aqueous solution. Elemental analyses (C, H, N) were performed with an Elementar Vario ELIII analyzer. IR spectra were measured on KBr pellets with a Nicolet Magna 750 FTIR spectrometer in the range of 400–4000 cm^{-1}. Magnetic susceptibilities of complexes **2**–**4**, **6**, and **11** were measured by using a Quantum Design SQUID magnetometer in the temperature range 6–300 K at a field of 1 T. The raw data were corrected for the magnetization of the sample holder.

Syntheses: *Caution!* Although we have experienced no problems in handling metal perchlorates, these should be handled with great caution because of the potential for explosion.

Synthesis of the $Cu(pic)_2$ Complex Precursor: The mononuclear precursor $[COH(NH_2)_2]_2[Cu(pic)_2(ClO_4)_2]$ was obtained according to the literature.[11]

Preparations of $[LnCu_2(pic)_4(H_2O)_6](ClO_4)_3\cdot H_2O$ [Ln = Sm (1), Nd (2), and Pr (3)]: A mixture of $Cu(pic)_2$ precursor (0.630 g, 1 mmol) and $Ln(ClO_4)_3$ aqueous solution (0.5 mL, 1 M) was added into C_2H_5OH/CH_3CN (volume ratio 1:1) solution (40 mL), followed by the addition of carbamide to adjust pH = 5, and the solution was stirred thoroughly at room temperature for 12 h and then filtered. The filtrate was concentrated to 20 mL and allowed to stand at room temperature. Deep-blue prismatic crystals were obtained after a few days. Yield: 52.5% (based on Sm) for **1**; 59.3% (based on Nd) for **2**; 62.8% (based on Pr) for **3**. IR (KBr): 1626 (vs), 1598 (vs), 1572 (s), 1481 (w), 1450 (w), 1404 (s), 1386 (m), 1298 (w), 1269 (w), 1144 (vs), 1115 (vs), 1089 (vs), 1053 (m), 1032 (w), 860 (w), 766 (m), 694 (m), 660 (w), 626 (m), 561 (w), 463 (w) cm^{-1} for **1**; 1625 (vs), 1598 (vs), 1569 (vs), 1481 (w), 1450 (w), 1404 (s), 1297 (w), 1269 (w), 1141 (vs), 1113 (vs), 1091 (vs), 1051 (m), 1031 (w), 860 (w), 767 (m), 692 (m), 659 (w), 626 (m), 561 (w), 461 (w) cm^{-1} for **2**. 1629 (vs), 1598 (vs), 1569 (s), 1481 (w), 1450 (w), 1404 (s), 1297 (m), 1268 (w), 1143 (vs), 1114 (vs), 1089 (vs), 1051 (m), 1030 (w), 858 (w), 765 (m), 694 (m), 657 (w), 626 (m), 563 (w), 460 (w) cm^{-1} for **3**. **1**: calcd. C 24.22, H 2.54, N 4.71; found C 24.25, H 2.58, N 4.70. **2**: calcd. C 24.34, H 2.89, N 4.73; found C 24.11, H 2.60, N 4.69. **3**: calcd. C 24.41, H 2.90, N 4.74; found C 24.32, H 2.57, N 4.67.

Preparations of $[Ln_2Cu_5(pic)_{10}(H_2O)_8](ClO_4)_6\cdot 2H_2O$ [Ln = Gd (4), Nd (5), Sm (6), Dy (7), Eu (8), Pr (9) and Yb (10)]: The second series complexes were prepared as mentioned above but the mole ratio of $Cu(pic)_2$ to $Ln(ClO_4)_3$ was changed to 3:1. Deep-blue prismatic crystals were obtained after a few days. Yield: 43.5% (based on Gd) for **4**; 48.3% (based on Nd) for **5**; 41.7% (based on Sm) for **6**; 35.6% (based on Dy) for **7**; 56.9% (based on Eu) for **8**; 42.6% (based on Pr) for **9**; 51.2% (based on Yb) for **10**. IR (KBr): 1631 (vs), 1599 (vs), 1570 (vs), 1481 (m), 1452 (w), 1404 (vs), 1390 (vs), 1352 (m), 1298 (s), 1267 (w), 1242 (w), 1144 (s), 1117 (vs), 1088 (vs), 1053 (s), 1033 (m), 864 (w), 831 (w), 771 (w), 762 (m), 713 (m), 696 (m), 659 (w), 626 (m), 565 (w), 469 (w) cm^{-1} for **4**; 1632 (vs), 1599 (vs), 1570 (vs), 1481 (m), 1452 (w), 1402 (s), 1389 (s), 1352 (m), 1298 (m), 1269 (w), 1242 (w), 1142 (s), 1115 (vs), 1090 (vs), 1051 (s), 1032 (m), 864 (w), 831 (w), 762 (m), 713 (m), 696 (m), 660 (w), 625 (m), 563 (w), 469 (w) cm^{-1} for **5**; 1627 (vs), 1599 (vs), 1570 (vs), 1481 (m), 1452 (w), 1402 (vs), 1389 (s), 1352 (s), 1297 (s), 1269 (m), 1242 (w), 1112 (vs), 1089 (vs), 1051 (s), 1032 (m), 863 (w), 831 (w),773 (m), 762 (m), 711 (m), 696 (m), 657 (w), 624 (m), 561 (w), 470 (w) cm^{-1} for **6**. 1627 (vs), 1602 (vs), 1569 (vs), 1482 (m), 1451 (w), 1402 (s), 1385 (s), 1354 (m), 1299 (m), 1265 (w), 1241 (w), 1143 (vs), 1115 (vs), 1088 (vs), 1052 (s), 1032 (m), 865 (w), 833 (w), 772 (m), 762 (m), 713 (m), 696 (m), 658 (w), 624 (m), 563 (w), 468 (w) cm^{-1} for **7**. 1630 (vs), 1600 (vs), 1570 (vs), 1480 (m), 1455 (w), 1402 (s), 1388 (s), 1354 (m), 1295 (m), 1267 (w), 1240 (w), 1145 (vs), 1110 (vs), 1092 (vs), 1054 (s), 1032 (m), 867 (w), 829 (w), 772 (m), 762 (m), 715 (m), 696 (m), 658 (w), 627 (m), 561 (w), 467 (w) cm^{-1} for **8**. 1633 (vs), 1598 (vs), 1571 (vs), 1481 (m), 1452 (w), 1401 (s), 1390 (s), 1352 (m), 1299 (m), 1269 (w), 1243 (w), 1154 (vs), 1111 (vs), 1091 (vs), 1052 (s), 1033 (m), 864 (w), 831 (w), 773 (m), 762 (m), 713 (m), 697 (m), 659 (w), 623 (m), 562 (w), 469 (w) cm^{-1} for **9**. 1632 (vs), 1601 (vs), 1573 (vs), 1479 (m), 1450 (w), 1410 (s), 1386 (s), 1286 (m), 1267 (w), 1242 (w), 1144 (vs), 1113 (vs), 1086 (vs), 1051 (m), 1032 (w), 862 (w), 837 (w), 762 (m), 694 (m), 650 (w), 625 (m), 561 (w), 463 (w) cm^{-1} for **10**. **4**: calcd. C 27.40, H 2.30, N 5.33; found C 27.35, H 2.31, N 5.31. **5**: calcd. C 27.67, H 2.32, N 5.38; found C 27.64, H 2.35, N 5.35. **6**: calcd. C 27.55, H 2.31, N 5.35; found C 27.53, H 2.34, N 5.30. **7**: calcd. C 27.29, H 2.29, N 5.30; found C 27.30, H 2.25, N 5.34. **8**: calcd. C 27.51, H 2.31, N 5.35; found C 27.52, H 2.30, N 5.29. **9**: calcd. C 27.75, H 2.33, N 5.39; found C 27.67, H 2.30, N 5.33. **10**: calcd. C 27.08, H 2.27, N 5.26; found C 27.15, H 2.30, N 5.23.

Preparation of $\{NdCu(pic)_2[CO(NH_2)_2]_4(H_2O)_3\}(ClO_4)_3\cdot[Cu(pic)_2]_2$ (11): The procedure of synthesis for the third series complex is similar to that for the first series compounds, but the mole ratio of $Cu(pic)_2$ to $Ln(ClO_4)_3$ is 4:1. Deep-blue prismatic crystals were obtained after a few days. Yield: 46.1% (based on Nd). IR (KBr): 1700 (m), 1660 (s), 1633 (vs), 1604 (vs), 1572 (m), 1480 (m), 1448 (w), 1406 (w), 1371 (s), 1358 (m), 1300 (m), 1290 (w), 1267 (w), 1242 (w), 1146 (s), 1117 (s), 1086 (s), 1049 (m), 1032 (w), 858 (w), 769 (w), 762 (w), 714 (w), 694 (m), 660 (w), 627 (m), 461 (w) cm^{-1}. Calcd. C 28.94, H 2.79, N 11.81; found C 28.89, H 2.77, N 11.78.

X-ray Crystallographic Studies. The crystal structures of the complexes were studied by single-crystal X-ray diffraction analyses. Data collections were performed at 293(2) K with a Siemens SMART CCD diffractometer for **1**–**3**, and **5**–**10** with graphite monochromatic Mo-K_α radiation (λ = 0.71073 Å),[16] with a Rigaku AFC7R diffractometer for **4** with graphite-monochromatic Mo-K_α radiation (λ = 0.71073 Å),[17] and a Rigaku Mercury CCD for **11** with graphite monochromatic Mo-K_α radiation (λ = 0.71073 Å).[18] The structures were solved by direct methods, the positions of the metal atoms were calculated by using the SIEMENS SHELXTL Version 5.0 package of crystallographic software.[19] The remaining non-hydrogen atoms were located by successive different Fourier syntheses. Hydrogen atoms were added according to theoretical models. The structures were refined using full-matrix least-squares refinement on F^2. All non-hydrogen atoms were refined anisotropically. Pertinent crystal data and structure refinement results for the complexes are listed in Table 1 for **1**–**3**, Table 2 for **4**–**6**, Table 3 for **7**–**9**, and Table 4 for **10** and **11**.

CCDC-237564 to -237574 (for **1**–**11**), contain the supplementary crystallographic data for this paper. These data can be obtained free of charge from The Cambridge Crystallographic Data Centre via www.ccdc.cam.ac.uk/data_request/cif.

Acknowledgments

This work was financially supported by the National Natural Science Foundation of China (20001007, 20131020), Natural Sciences Foundation of Fujian Province (2003I031).

[1] a) D. M. J. Doble, C. H. Benison, A. J. Blake, D. Fenske, M. S. Jackson, R. D. Kay, W. S. Li, M. Schröder, *Angew. Chem. Int. Ed.* **1999**, *38*, 1915–1918; b) J. Lisowski, P. Starynowicz, *Inorg. Chem.* **1999**, *38*, 1351–1355; c) J. P. Costes, F. Dahan, A. Dupuis, J. P. Laurent, *Inorg. Chem.* **1997**, *36*, 3429–3433; d) C. Benelli, D. Gatteschi, *Chem. Rev.* **2002**, *102*, 2369–2387; e) G. Li, T. Akitsu, O. Sato, Y. Einaga, *J. Am. Chem. Soc.* **2003**, *125*, 12396–12397; f) H. Z. Kou, B. C. Zhou, S. Gao, R. J. Wang, *Angew. Chem. Int. Ed.* **2003**, *42*, 3288–3291; g) M. Sakamoto, K. Manseki, H. Okawa, *Coord. Chem. Rev.* **2001**, *219–221*, 379–414.

[2] a) H. Z. Kou, S. Gao, J. Zhang, Z. H. Wen, G. Su, R. K. Zheng, X. X. Zhang, *J. Am. Chem. Soc.* **2001**, *123*, 11809–11810; b) B. Q. Ma, S. Gao, G. Su, G. X. Cu, *Angew. Chem. Int. Ed.* **2001**, *40*, 434–437.

[3] T. Kido, Y. Ikuta, Y. Sunatsuki, Y. Ogawa, N. Matsumoto, *Inorg. Chem.* **2003**, *42*, 398–408.

[4] a) A. Bencini, C. Benelli, A. Caneschi, A. Dei, D. Gatteschi, *Inorg. Chem.* **1986**, *25*, 572–575; b) A. Bencini, C. Benelli, A. Caneschi, R. L. Carlin, A. Dei, D. Gatteschi, *J. Am. Chem. Soc.* **1985**, *107*, 8128–8136; c) S. R. Bayly, Z. Xu, B. O. Patrick, S. J. Rettig, M. Pink, R. C. Thompson, C. Orvig, *Inorg. Chem.* **2003**, *42*, 1576–1583.

[5] a) C. Benelli, A. Caneschi, D. Gatteschi, O. Guillou, L. Pardi, *Inorg. Chem.* **1990**, *29*, 1750–1755; b) T. Kido, S. Nagasato, Y. Sunatsuki, N. Matsumoto, *Chem. Commun.* **2000**, 2113-2114.

[6] M. Andruk, L. Ramade, E. Codjovi, O. Guillou, O. Kahn, J. C. Trombe, *J. Am. Chem. Soc.* **1993**, *115*, 1822–1829.

[7] a) R. Georges, O. Kahn, O. Guillou, *Phys. Rev. B* **1994**, *49*, 3235–3242; b) S. Wang, Z. Pang, M. J. Wagner, *Inorg. Chem.* **1992**, *31*, 5381–5388.

[8] a) O. Guillou, O. Kahn, R. L. Oushoorn, *Inorg. Chim. Acta* **1992**, *198–200*, 119–131; b) O. Guillou, P. Bergerat, O. Kahn, E. Bakalbassis, K. Boubekeur, P. Batail, M. Guillot, *Inorg. Chem.* **1992**, *31*, 110–114; c) O. Guillou, R. L. Oushoorn, O. Kahn, K. Boubekeur, P. Batail, *Angew. Chem. Int. Ed. Engl.* **1992**, *31*, 626–628; d) C. Daiguebonne, O. Guillou, M. L. Kahn, O. Kahn, R. L. Oushoorn, K. Boubekeur, *Inorg. Chem.* **2001**, *40*, 176–178; e) Z. He, C. He, E. Q. Gao, Z. M. Wang, X. F. Yang, C. S. Liao, C. H. Yan, *Inorg. Chem.* **2003**, *42*, 2206–2208; f) H. Z. Kou, B. C. Zhou, R. J. Wang, *Inorg. Chem.* **2003**, *42*, 7658–7665; g) B. Zhao, P. Cheng, Y. Dai, C. Cheng, D. Z. Liao, S. P. Yan, Z. H. Jiang, G. L. Wang, *Angew. Chem. Int. Ed.* **2003**, *42,* 934–936.

[9] A. J. Blake, R. O. Gould, P. E. Y. Milne, R. E. P. Winpenny, *J. Chem. Soc. Chem. Commun.* **1992**, 522–524.

[10] a) J. G. Mao, L. Song, X. Y. Huang, J. S. Huang, *Polyhedron* **1997**, *16*, 963–966; b) J. G. Mao, L. Song, J. S. Huang, *J. Chem. Cryst.* **1998**, *28*, 475–479; c) J. G. Mao, J. S. Huang, J. F. Ma, J. Z. Ni, *Transit. Metal Chem.* **1997**, *22,* 277–280; d) Y. Cui, G. Chen, J. Ren, Y. T. Qian, J. S. Huang, *Inorg. Chem.* **2000**, *39*, 4165–4168; e) X. Zhang, Y. Cui, F. K. Zheng, J. S. Huang, *Chem. Lett.* **1999**, 1111–1112.

[11] G. H. Guo, G. C. Guo, G. W. Zhou, M. S. Wang, L. Z. Cai, A. Q. Wu, J. S. Huang, *Chinese J. Inorg. Chem.* **2003***, 19*, 95–98.

[12] a) S. Kiani, A. Tapper, R. J. Staples, P. Stavropoulos, *J. Am. Chem. Soc.* **2000**, *122*, 7503–7517; b) H. J. Eppley, S. M. Aubin, W. E. Streb, J. C. Bollinger, D. N. Hendrickson, G. Christou, *Inorg. Chem.* **1997**, *36*, 109–115; c) D. M. Stearns, W. H. Armstrong, *Inorg. Chem.* **1992**, *31*, 5178–5184; d) J. Kay, J. W. Mcore, M. D. Glick, *Inorg. Chem.* **1972**, *11*, 2818–2827; e) J. F. Ma, N. H. Hu, J. Z. Ni, *Polyhedron* **1996**, *15*, 1797–1799.

[13] Q. D. Liu, S. Gao, J. R. Li, Q. Z. Zhou, K. B. Yu, B. Q. Ma, S. W. Zhang, X. X. Zhang, T. Z.Jin, *Inorg. Chem.* **2000**, *39*, 2488–2492.

[14] P. Starynowicz, *Acta Crystallogr.*, *Sect. C.: Cryst. Struct. Commun.* **1991**, *47*, 294–297.

[15] M. L. Kahn, C. Mathoniere, O. Kahn, *Inorg. Chem.* **1999**, *38*, 3692–3697.

[16] *Siemens SHELXTL™ Version 5 Reference Manual*, Siemens Energy & Automation Inc., Madison, Wisconsin, USA, **1994**.

[17] a) *Rigaku WinAFC*, Rigaku Corporation, **2002**; b) *Rigaku Crystal Structure Version 3.10*, Rigaku Corporation and Rigaku/MSC, **2002**.

[18] *Rigaku CrystalClear 1.35 Software User's Guide for the Rigaku R-Axis, and Mercury and Jupiter CCD Automated X-ray Imaging System*, Rigaku Molecular Structure Corporation, Utah, USA, **2002**.

[19] *Siemens SHELXTL Version 5.0, Reference Manual*, Siemens Analytical X-ray Instruments Inc., Madison, Wisconsin, USA, **1995**.

Received: August 4, 2004